Kinetics and Catalysis, Vol. 44, No. 4, 2003, pp. 499–512. Translated from Kinetika i Kataliz, Vol. 44, No. 4, 2003, pp. 548–562.

Reactions of Neutral and Charged Molybdenum Oxide Clusters with Low-Molecular-Weight Alcohols in a Gas Phase Studied by Ion Cyclotron Resonance

V. B. Goncharov

Boreskov Institute of Catalysis, Siberian Division, Russian Academy of Sciences, Novosibirsk, 630090 Russia

Received December 12, 2001

Abstract—A set of oxygen-containing molybdenum oxide clusters Mo_xO_y (x = 1–3; y = 1–9) was obtained with the use of a combination of a Knudsen cell and an ion trap cell. The reactions of positively charged clusters with C_1–C_4 alcohols were studied using ion cyclotron resonance. The formation of a number of organometallic ions, the products of initial insertion of molybdenum oxide ions into the C–O and C–H bonds of alcohols, and polycondensation products of methanol and ethanol were found. The reactions of neutral molybdenum oxide clusters Mo_xO_y (x = 1–3; y = 1–9) with protonated C_1–C_4 alcohols and an ammonium ion were studied. The following limits of proton affinity (*PA*) were found for neutral oxygen-containing molybdenum clusters: (MoO) < 180, (Mo_2O_4, Mo_2O_5, and Mo_3O_8) = 188 ± 8, *PA*(MoO_2) = 202 ± 5, *PA*(MoO_3, Mo_2O_6, and Mo_3O_9) > 207 kcal/mol.

INTRODUCTION

Supported molybdenum-containing catalysts in oxide and sulfide forms are widely used in various branches of chemistry and petroleum processing [1–3]. Large-scale processes such as the hydrofining of oil fractions; the hydrogenolysis of C–S, C–N, and C–O bonds [4]; the demetalation of petroleum [5]; and the partial oxidation of organic compounds are performed with the participation of these catalysts [3]. Another area of application of molybdenum oxides is the hydrogenation and dehydrogenation of hydrocarbons [6] and the polymerization and metathesis of olefins [7, 8].

The mechanisms of oxidation reactions with the participation of molybdenum trioxide often include the exothermic steps of oxygen transfer from the oxometallic groups of a catalyst to an organic substrate [3]. It is believed that the most important factors responsible for the catalytic activity of molybdenum oxide are the oxidation state of molybdenum and the occurrence of free coordination sites at the oxide surface [9].

A great body of data on the activation of C–H and C–C bonds in hydrocarbons by transition metal ions has been accumulated in the past two decades [10]. It is assumed that the interaction of isolated (i.e., unbound to ligands) metal ions with hydrocarbon molecules occurs through the following four steps (Fig. 1):

(1) The formation of an amorphous complex because of a collision followed by the interaction of a metal ion with the dipole of a neutral molecule induced by this ion.

The energy of this interaction for a singly charged ion and a hydrocarbon (C_3–C_4) is ~10–15 kcal/mol (even at an initial energy of the ion–dipole system of the order of kT). This energy is sufficient to overcome internal barriers and insert the metal ion into a C–H or C–C bond of the hydrocarbon.

(2) The oxidative addition of the metal ion at a C–H (or C–C) bond of the hydrocarbon.

In this case, the cleavage of a C–H (or C–C) bond and the formation of two new M^+–C and M^+–H bonds (where M^+ is the metal ion) takes place. Because the method of ion cyclotron resonance (ICR) makes it possible to observe the occurrence of only exothermic reactions in a gas phase, the energy of final products, as well as all the intermediate compounds, should be lower than the energy of initial reactants. That is, the total energy of the formed M^+–C and M^+–H bonds should be higher than the energy of the initial C–H (or C–C) bond of the hydrocarbon.

(3) The transfer of a β-hydrogen atom to the metal ion (β-shift) with the formation of a dihydride–metal–alkene complex (H–M^+(H)–R).

A common trend is that the β-shift of hydrogen from a secondary carbon atom occurs more readily than from a primary carbon atom. In the case of branched hydrocarbons, the transfer of a hydrocarbon fragment, for example, the CH_3 group, is also possible.

(4) The elimination of a hydrogen (or alkane) molecule and the formation of the final metal–alkene complex.

In this case, the metal ion can attack the next C–H or C–C bond with the formation of secondary reaction products. A comparison of data on the bond energies of metal ions with various ligands demonstrated that the Cr^+ ion forms weak binary metal–carbon and metal–hydrogen bonds; because of this, the step of insertion

0023-1584/03/4404-0499$25.00

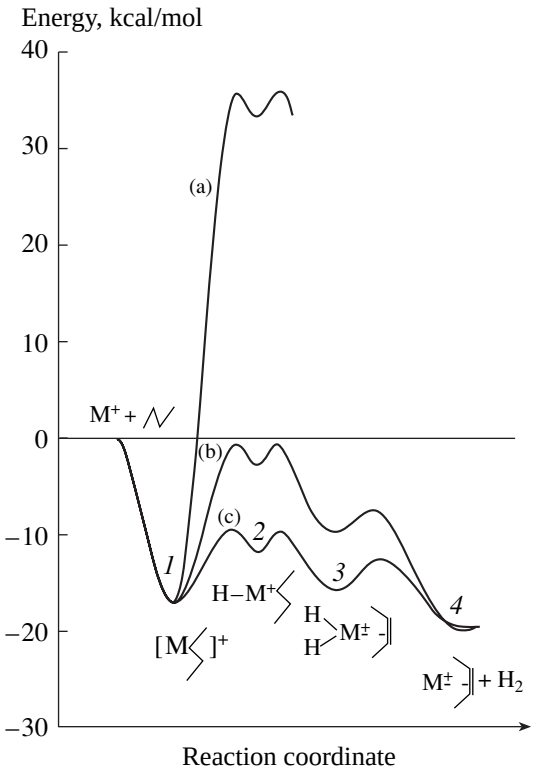

Fig. 1. Assumed reaction paths in the dehydrogenation of the *n*-butane molecule with (a) Cr^+, (b) Mo^+, and (c) W^+ ions: *1–4* are the steps of the interaction of the metal ions with hydrocarbons (see the text).

into the C–H bond (step *2*) is strongly endothermic. It is likely that in the reaction with Mo^+ ions the step of addition at the C–H bond is almost thermally neutral (Fig. 1), whereas W^+ ions react rapidly with butane to form dehydrogenation products [11].

The reactivity of metal oxide ions significantly depends on the bond energy $D_0(M^+–O)$. Thus, the reactivity of FeO^+ [12], CrO^+ [13], and OsO^+ [14], which have small (70–85 kcal/mol) bond energies with oxygen, increases, as compared with "naked" metal ions, because of the appearance of new reaction paths with the participation of oxygen (the formation of OH groups and water and hydrocarbon oxidation). However, the reactivity of VO^+, which has a very strong bond (134 kcal/mol) with oxygen, is lower than that of the V^+ ion [15]. In this case, oxygen cannot participate in oxidation reactions; it only occupies one coordination site at the metal ion. Because of the occurrence of ion–molecule reactions, the heat effect of reaction is redistributed within the ion–molecule complex over all the degrees of freedom. A common trend is that, if the dissipation of an excessive energy from the ion–molecule complex is hindered, the subsequent occurrence of reactions that result in the products of multiple dehydrogenation is feasible. Therefore, the problem of the presence or absence of excitation is closely related to reaction conditions or, more precisely, to the intramolecular and intermolecular mechanisms of energy relaxation. Even at an initial ion energy of the order of *kT* (i.e., thermal), the energy released can be conserved in reaction products as kinetic, vibrational, or electronic excitation. This excitation can result in the acceleration of consecutive slow steps. In contrast, relaxation processes occur very rapidly at solid surfaces, so that the energy of an exothermic reaction cannot be used for performing the subsequent endothermic steps.

The unique catalytic properties of molybdenum oxide gave impetus to research into the reactivity of Group VI ions in a gas phase.

Thus, the interactions of Cr^+, Mo^+, and W^+ ions with alkanes and alkenes were studied using ion-beam spectroscopy and ICR. It was found that the Mo^+ and W^+ ions can activate the C–H bonds of hydrocarbons to form organometallic products of dehydrogenation [11, 16].

Cassdy and McElvany [17] studied the gas-phase reactions of Mo^+, MoO^+, and MoO_2^+ ions with low-molecular-weight alkanes and alkenes using ICR [17]. The formation of hydrocarbon dehydrogenation products was also the predominant channel of these reactions. Because the MoO^+ and MoO_2^+ ions possessed sufficiently strong bonds $D_0(Mo^+–O)$ and $D_0(MoO^+–O)$ (Table 1), the presence of oxygen had no effect on the reactivity of the MoO^+ ion. The reactivity of the MoO_2^+ ion somewhat increased; in addition to dehydrogenation reactions, the products of C–C bond cleavage in hydrocarbons were detected in the case of this ion. It is believed that the main factor affecting the reactivity of ions is the number of accessible coordination sites.

The gas-phase reactions of Fe^+, Cr^+, and Mo^+ ions generated by multiphoton ionization with a number of aliphatic alcohols were studied by ICR [18]. These ions react with alcohols via the following three main channels: (1) insertion into the C–O bond (dehydration), (2) insertion into the C–H and O–H bonds (dehydrogenation), and (3) C–C insertion. The Mo^+ ion reacts to cause mainly single or multiple dehydrogenation. The dehydrogenation and insertion into C–C bonds were observed only in branched alcohols.

Previously [19–23], we studied the preparation of molybdenum oxide cluster ions $Mo_xO_y^+$ (x = 1–5; y = 1–15) in a gas phase and their reactions with small molecules. It was found that large oxides (x = 4, 5) were unstable under reaction conditions. Molybdenum oxide ions reacted with *cis*-C_3H_6 by inserting into C–C and C–H bonds of the hydrocarbon to form carbene species and dehydrogenation products. In this case, the reactivity of the ions was independent of the number of metal ions in the cluster [23].

It this work, an attempt was made to study the reactivity of molybdenum oxide ion clusters $Mo_xO_y^+$ (x = 1–3; y = 1–9) in reactions with methanol, ethanol, 2-butanol,

Table 1. Bond energies in neutral and charged molybdenum oxides, ionization potentials (*PI*), low-energy structures of molybdenum oxides, and energy (in terms of an atom)

Oxide	*PI*, kcal/mol	Bond energy, kcal/mol					Optimum structure	Energy in terms of an atom, arb. u.
		reference data [24]		calculated data		experimental M^+–O		
		M–O	M–MoO_3	M^+–O	M^+–MoO_3			
MoO	173	120	–	98.5	–	<151 [28] 118 ± 2 [29]		–80.1
MoO_2	217	158	–	121	–	>118 [28] <127 [30] 131 ± 5 [29]		–92.5
MoO_3	277	143	–	83	–	> 85 < 118 [28] <127 [30] 62 ± 7 [28]	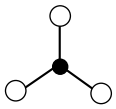	–89.7
Mo_2O_4	–	–	–	–	–	–	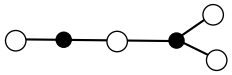	–85.8
Mo_2O_5	238	–	–	–	–	–	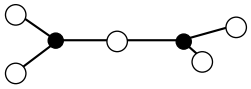	–90.8
Mo_2O_6	280	104	114	56	112	<127 [30]	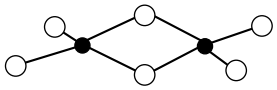	–89.0
Mo_3O_8	282	–	–	–	–	–	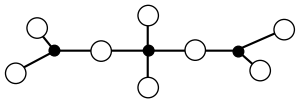	–88.7
Mo_3O_9	277	53	86	58	86	<127 [30]	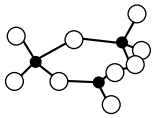	–94.5
Mo_4O_{11}	–	–	–	–	–	–	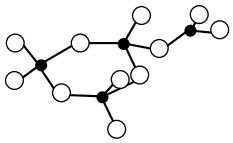	–82.6
Mo_4O_{12}	277	–	73	–	73	–	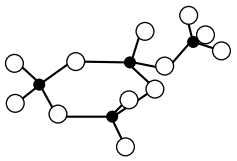	–85.6
Mo_5O_{15}	277	–	76	–	78	–	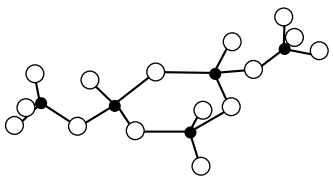	–83.6

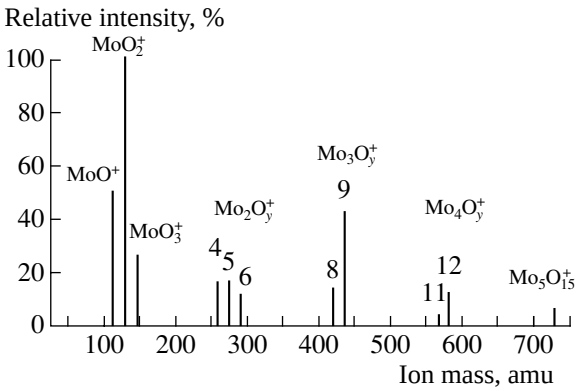

Fig. 2. Mass spectrum of the positive ions of molybdenum oxides obtained by the evaporation of $^{98}MoO_3$ from a Knudsen effusion source; 600 K (figures at the peaks correspond to the value of y in the formula $Mo_xO_y^+$).

and 2-methyl-2-propanol (*tert*-butanol) and the protonation reactions of neutral molybdenum oxide clusters with gas-phase bases.

EXPERIMENTAL

The experiments were performed on a Bruker-Spectrospin CMS-47 ICR mass spectrometer with an Oxford Instruments 4.7-T vertical cryomagnet equipped with a cubic ion trap cell (33 mm). The vacuum system of the spectrometer was pumped out with an ion pump (pump speed of 160 l/s) to a base pressure of $(1–2) \times 10^{-7}$ Pa (at room temperature of the plates of the ion trap cell). A Bayard–Alpert ionization gauge was used for pressure measurements. Molybdenum oxide clusters were generated by evaporating molybdenum trioxide from a Knudsen quartz cell. The Knudsen cell equipped with a bifilar heater was mounted on the holding plate of an ICR cell on the anode side. This design provided the heating of the cell over a temperature range of 300–900 K without considerable gas evolution and magnetic field destabilization. The temperature control was performed with a Chromel–Alumel thermocouple using a calibration function (temperature–heater current); α-Al_2O_3 powder was used as a reference substance. The area ratio was $S/s > 1500$, where S is the internal surface area of the Knudsen cell, and s is the area of the orifice. The dry isotope of molybdenum trioxide (VO Izotop) was enriched in the ^{98}Mo isotope by 97%. The use of a monoisotopic sample (natural abundance of molybdenum isotopes: ^{92}Mo (61.5%), ^{94}Mo (38.3%), ^{95}Mo (65.9%), ^{96}Mo (39.6%), ^{98}Mo (100.0%), and ^{100}Mo (39.9%) simplified the mass spectra and increased the sensitivity of the method to heavy ions by one order of magnitude.

Molybdenum oxide ions were generated from molybdenum trioxide vapor using electron impact (70 eV). An alcohol pressure in the vacuum system was usually equal to $\sim(1–2) \times 10^{-5}$ Pa. The ICR spectrum was excited using a standard sequence of electron pulses, which was repeated dozens of times to obtain a reasonable level of signal-to-noise ratios. The ICR spectra were measured in a Fourier transform mode. The mass window limits varied from 2 to 10 amu depending on the test mass range. The accuracy of measuring ratios between ion products was 10%.

A double-resonance technique was used for studying the mechanisms of ion–molecule reactions in a gas phase. This technique makes it possible to remove initial ions with a specified mass-to-charge ratio at the beginning of each particular experiment. In this case, the observed changes in ICR spectra provided information on the reactions occurring.

Figure 2 demonstrates the mass spectrum of molybdenum oxide ions (70 eV) obtained by evaporating molybdenum trioxide $^{98}MoO_3$ at 600 K. It can be seen that molybdenum oxide cluster ions $Mo_xO_y^+$, which contained different numbers of metal and oxygen atoms, were formed. At the beginning of each particular experiment, foreign ions were completely removed using the double-resonance technique; the remaining ions with a chosen value of m/z reacted with neutral molecules; next, the reaction products were detected.

The double-resonance technique was also used for the collision-induced dissociation (CID) of ion products. In this case, the parent ion was accelerated to hundreds of electronvolts; it collided with a neutral gas (Ar). Based on the detected ionic fragments of the parent ion, conclusions about the initial structure of the ion on the empirical formula level can be drawn.

RESULTS AND DISCUSSION

Bond Energies in Molybdenum Oxide Ions: The Structure of Molybdenum Oxides

The kinetic method of the destructive addition of ligands was used for the experimental determination of metal–ligand bond energies. Let us consider the reaction of a metal ion M^+ with a neutral molecule L_1L_2:

$$M^+ + L_1L_2 \longrightarrow ML_1^+ + L_2. \qquad (I)$$

Because only exothermic reactions can be observed by ICR, the formation of ML_1^+ ions indicates that the lower limit of the ion bond strength $D_0(M^+–L_1)$ is greater than the bond strength in the neutral molecule $D_0(L_1–L_2)$. However, the absence of the products of reaction (I) cannot always be considered as evidence for the fact that the upper limit of the bond $D_0(M^+–L_1)$ is lower than $D_0(L_1–L_2)$ because of the conceivable presence of a great energy barrier.

The bond energies of oxygen atoms in molybdenum oxide ions were evaluated using the following thermodynamic cycle:

$$\begin{array}{ccc} M^+–L & \xrightarrow{D_0(ML^+)} & M^+ + L \\ \uparrow PI(ML^+) & & \uparrow PI(M^+) \\ M–L & \xrightarrow{D_0(ML)} & M + L \end{array} \qquad \text{(II)}$$

$$D_0(M^+–L) = D_0(M–L) + PI(M) – PI(ML),$$

where *PI* is ionization potential.

The calculated values of $D_0(M^+–L)$ are given in Table 1 with the bond energies of oxygen in neutral molecules and their ionization potentials. The bond energies and ionization potentials (*PI*) of neutral molecules were taken from [24]. Data presented in Table 1 suggest that molybdenum oxide ions with the retained stoichiometry MoO_3 exhibited the least strong bond with oxygen. Thus, it would be expected that the reactivity of ions with the least energy of the molybdenum–oxygen bond, that is, $(MoO_3)_x^+$, in reactions with alcohols will be maximum.

The structures of various molybdenum oxides were studied using a simple model of pair potentials. Molecular geometries resulted from the minimization of the total energy of a molecule with the use of the following potential function:

$$U_t = U_{MO} + U_{MM} + U_{OO}, \qquad (1)$$

where U_t is the total energy of the system; U_{MO} is the Coulomb energy of the interaction of molybdenum and oxygen; and U_{OO} and U_{MM} are the energies of the interactions of oxygen and molybdenum atoms with each other, respectively. The energy was calculated as the sum of the Coulomb interaction and the Born–Meyer repulsion

$$U_{ij} = \frac{q_i q_j}{r_{ij}} + A\exp\left[-\frac{r_{ij}}{\rho}\right], \qquad (2)$$

where U_{ij} is the Coulomb energy of the interaction of *i*th and *j*th atoms; r_{ij} is the internuclear distance for each pair of atoms; q_i and q_j are the formal atomic charges determined from the stoichiometry; A and ρ are variable parameters, which were chosen so that bond lengths in a monomer and in the bulk molybdenum trioxide were retained. The values of $A = 2256$ e^2/Å (e is the electron charge) and $\rho = 0.181$ Å were used in the calculations. The absence of the Mo–Mo bond was assumed in the calculations. A similar model was used for determining the geometries of cobalt and titanium oxide ions [25–27]. The results of the calculations demonstrated that the oxygen-deficient and stoichiometric oxides can exhibit different structures, which are responsible for differences in reactivity.

Several low-energy isomers were found for each molybdenum oxide. Table 1 summarizes optimum structures for all the molybdenum oxides together with the calculated total energies of the molecules and energies in terms of a cluster atom.

Among the structures presented, MoO_2^+ and MoO_3^+ ions contain structurally and energetically equivalent oxygen atoms.

An exact quantum-chemical calculation of the structure and bond energy of the MoO_3^+ ion, which was performed by Schwartz *et al.* [29], demonstrated that the MoO_3^+ ion ($^2A_2$) exhibits C_{3v} symmetry. All the oxygen atoms are equivalent (see structure **I**); that is, deviations from the corresponding data for the neutral molecule of MoO_3 are small ($r_{Mo–O} = 1.70$ Å).

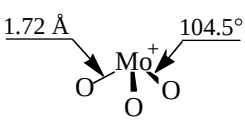

I

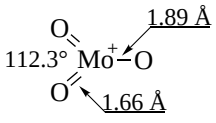

II

The energy of structure **II** of MoO_3^+ ($^2B_2$) is insignificantly higher (by 4 kcal/mol) than that of structure **I**. However, The symmetry is reduced to C_{3v}, and oxygen atoms are structurally and energetically nonequivalent; this is most clearly pronounced in the structures of dimers and trimers.

The structures of dimers and trimers (Table 1) contain bridging and terminal oxygen atoms. The (bridging) oxygen atoms of Mo–O–Mo corner groups are more strongly bound; the highest electron density is concentrated at these atoms because of the weaker d_π–P_π reverse interaction. It is believed that these atoms are the localization sites of external protons in heteropoly acids [31, 32].

Among the clusters presented, the $Mo_3O_9^+$ ion exhibit a cyclic structure, which is the thermodynamically most favorable; the cyclic Mo_3O_9 fragment is also retained in the structures of $Mo_4O_{12}^+$ and $Mo_5O_{15}^+$ ions. According to gas electron diffraction data for neutral molybdenum trioxide Mo_3O_9 [33], the Mo–O distances in this structure are as follows: $Mo–O_{(terminal)}$ of 1.67 Å and $Mo–O_{(bridging)}$ of 1.89 Å. Because of its unique structure, the $Mo_3O_9^+$ ion would be expected to exhibit reactivity different from that of monomers and dimers.

Reactions of Neutral Molybdenum Oxide Clusters: Proton Affinity

ICR spectrometry is among the few techniques that can be used to determine the acidity or basicity of unsolvated molecules [34]. The other techniques are ordinary high-pressure mass spectrometry, where two molecules compete for a proton, similarly to the case of the ICR method, and a combination of the heats of formation of other substances, in which the proton affinity

can be calculated from mass-spectrometric data on the appearance energy or other sources. The proton affinity (*PA*) of a molecule (M) is defined as the negative of the enthalpy change for the reaction

$$M + H^+ \longrightarrow MH^+ \quad \text{(III)}$$

in a gas phase. The enthalpy change for reaction (III) is

$$-PA = \Delta H = \Delta H_f(MH^+) - \Delta H_f(M) - \Delta H_f(H^+). \quad (3)$$

The enthalpy of formation $\Delta H_f(H^+)$ of the H^+ ion is equal to 365.48 kcal; the enthalpies of formation of hundreds of small molecules are known [30], so the determination of proton affinity depends only on the capabilities of measuring $\Delta H_f(MH^+)$.

Ion cyclotron double resonance experiments provide an opportunity to determine narrow ranges of the proton affinities of simple molecules. The principle of double resonance is that a radiofrequency (RF) pulse is used not only for the excitation of cyclotron motion followed by the detection of ions but also for the translational excitation of selected ions. The use of this technique makes it possible to perform tandem mass-spectrometric experiments in an ICR spectrometer.

Double resonance pulses can be used for the removal of specified ions from a cell and/or for the translational excitation of ions and for the accomplishment of exothermic reactions. Measurements are indirect, and they require knowledge of the proton affinities of other molecules. To determine the limits of ΔH_f for the MH^+ ion, let us consider the acid–base reaction

$$M_1 + M_2H^+ \longrightarrow M_1H^+ + M_2. \quad \text{(IV)}$$

The enthalpy of reaction (IV) is

$$\Delta H = \Delta H_f(M_1H^+) + \Delta H_f(M_2) - \Delta H_f(M_1) - \Delta H_f(M_2H^+). \quad (4)$$

The enthalpy of the molecule of interest is

$$\Delta H_f(M_1H^+) = \Delta H - \Delta H_f(M_2) + \Delta H_f(M_1) + \Delta H_f(M_2H^+). \quad (5)$$

The enthalpy of reaction (IV) is unknown; however, its sign can be determined from the measurement of a double resonance signal as a function of the irradiating RF field. Among terms in the right-hand side of Eq. (4), only the first term is unknown. If it can be considered negative based on ICR experiments, the sum of the other three terms determines the upper limit of the enthalpy of formation. If the M_1H^+ ion serves as a parent reactant ion in another reaction of this type and gives a negative signal of double resonance, the lower limit of the enthalpy of formation of the M_1H^+ ion can be established. Very narrow limits for determining this value can be established with a careful selection of reactions.

The above method is widely used. The direct measurement of the equilibrium constants of gas acid–base reactions in an ion trap cell is also feasible. It gives results that are more accurate; however, unfortunately, it is restricted by a narrow dynamic range of ICR spectrometers (~10^3).

By now, the proton affinities of several hundreds of molecules, primarily, organic, have been measured. The measurement of this quantity for inorganic substances is associated with considerable difficulties; the main problem is the sublimation of solid substances.

The proton affinity was determined as described below. Alcohol vapor or ammonia was admitted to the vacuum system of an ICR spectrometer with an operating effusion source. Next, the electron impact (70 eV) resulted in the ionization of all neutral molecules in the volume of the ICR cell. Subsequently, molybdenum-containing ions were completely removed by double resonance pulses; in this case, only the parent ions of alcohols or ammonia remained. In this case, the following reactions occurred:

$$ROH^+ + ROH \longrightarrow ROH_2^+ + RO^\bullet, \quad \text{(V)}$$

$$ROH_2^+ + Mo_xO_y \longrightarrow ROH + Mo_xO_yH^+, \quad \text{(VI)}$$

where R is the alkyl residue of the alcohol.

The occurrence of the reaction via this path was tested using the double resonance technique. Knowing the proton affinity of the molecule of base B, the upper and lower limits of the proton affinity can be evaluated for various molybdenum oxides.

Table 2 summarizes data on protonation reactions and the proton affinities of various bases taken from [35].

Table 2. Reactions of proton transfer from protonated alcohols and the ammonium ion to oxygen-containing molybdenum clusters and the proton affinities of various bases [35]

Base	*PA*, kcal/mol	MoO	MoO_2	MoO_3	Mo_2O_4	Mo_2O_5	Mo_2O_6	Mo_3O_8	Mo_3O_9
CH_3OH	180	–	+	+	+	+	+	+	+
C_2H_5OH	186	–	+	+	±	±	+	±	+
iso-C_4H_9OH	197	–	+	+	–	–	+	–	+
tert-C_4H_9OH	206	–	±	+	–	–	+	–	+
NH_3	207	–	–	+	–	–	+	–	+

Molybdenum oxide molecules with the stoichiometry MoO_3 were protonated in the presence of all the bases. Thus, they exhibited high proton affinity:

$$PA(MoO_3, Mo_2O_6, Mo_3O_9) > 207 \text{ kcal/mol}.$$

The MoO_2 molecules were protonated by all the acids except for NH_4^+, and the reaction with *tert*-butanol was very slow. The value of $PA(MoO_2)$ should be close to $PA(tert\text{-}C_4H_9OH) = 206$ kcal/mol. According to our estimations, $PA(MoO_2) = 202 \pm 5$ kcal/mol.

The Mo_2O_4, Mo_2O_5, and Mo_3O_8 molecules were protonated very slowly in the presence of ethanol. Their *PA* values should be close to $PA(C_2H_5OH) = 186$ kcal/mol:

$$PA(Mo_2O_4, Mo_2O_5, Mo_3O_8) = 188 \pm 8 \text{ kcal/mol}.$$

Finally, the MoO molecules were not protonated in the presence of any acid; this fact suggests a low *PA* value:

$$PA(MoO) < 180 \text{ kcal/mol}.$$

More accurate proton affinity values could be obtained by studying in detail the equilibrium between protonated and unprotonated species. However, this was impossible because the partial pressures of individual molybdenum oxides cannot be determined.

Reactions with Methanol

Four main reactions occurred in the interaction of molybdenum oxide ions with methanol in a gas phase. First, the reactions of formaldehyde and water elimination and methanol oxidation to formaldehyde took place:

$$Mo_xO_y^+ + CH_3OH \longrightarrow Mo_xO_yH_2^+ + CH_2O, \quad \text{(VII)}$$

$$Mo_xO_y^+ + CH_3OH \longrightarrow Mo_xO_yCH_2^+ + H_2O. \quad \text{(VIII)}$$

Second, $Mo_xO_yCH_3^+$ and $Mo_xO_yCH_4^+$ ions were formed:

$$Mo_xO_y^+ + CH_3OH \longrightarrow Mo_xO_yCH_3^+ + \dot{O}H, \quad \text{(IX)}$$

$$Mo_xO_y^+ + CH_3OH \longrightarrow Mo_xO_yCH_4^+ + O^{\bullet}. \quad \text{(X)}$$

Moreover, $Mo_3O_9^+$ ions can react with several molecules of methanol to form a longer carbon chain. Table 3 demonstrates the distribution of reaction products.

Previously [18], it was found that Mo^+ reacts with methanol to quantitatively dehydrogenate it to formaldehyde. The products of reactions that occur with the initial activation of C–O bonds were not detected.

Reactions of MoO^+

The addition of an oxygen atom somewhat changed the reactivity of the metal ion in reactions with methanol. MoO^+ also dehydrogenated methanol; however, the elimination of formaldehyde rather than a hydrogen molecule, as in the case of Mo^+, was preferable.

$$MoO^+ + CH_3OH \longrightarrow MoOH_2^+ + CH_2O. \quad \text{(XI)}$$

It is interesting that reaction (XI) is analogous to the oxidative dehydrogenation of methanol to formaldehyde, which occurs on heterogeneous catalysts contain-

Table 3. Distribution of products (%) of the reactions of $Mo_xO_y^+$ ions with methanol and CD_3OH

Alcohol	Reaction products	MoO^+	MoO_2^+	MoO_3^+	$Mo_2O_4^+$	$Mo_2O_5^+$	$Mo_2O_6^+$	$Mo_3O_8^+$	$Mo_3O_9^+$
CH_3OH	$Mo_xO_yH_2^+ + CH_2O$	100	16	14	28	25	6	15	21
	$Mo_xO_yCH_2^+ + H_2O$	–	15	–	38	17	33	18	–
	$Mo_xO_yCH_3^+ + OH$	–	32	54	34	17	61	19	50
	$Mo_xO_yCH_4^+ + O$	–	37	32	–	41	–	48	–
	Polycondensation products	–	–	–	–	–	–	–	29
CD_3OH	$Mo_xO_yHD^+ + \ddot{e}D_2O$	100	10	14	29	16	35	20	27
	$Mo_xO_yCD_4^+ + HDO$	–	17	–	29	28	27	15	–
	$Mo_xO_yCD_3^+ + OH$	–	38	43	42	28	38	15	44
	$Mo_xO_yCD_3H^+ + O$	–	35	43	–	28	–	50	–
	Polycondensation products	–	–	–	–	–	–	–	29

ing molybdenum oxide [36]. It is assumed that the real catalytic process occurs in two steps. The first step is methanol oxidation accompanied by surface reduction. Reaction (XI) is a gas-phase model of this step. The second step is surface oxidation with atmospheric air, which is analogous to the oxidation of $MoOH_2^+$ with oxygen. The possibility of catalytic oxidation reactions occurring in a gas phase in the presence of transition metal oxide ions was demonstrated previously [28]. Because the Mo^+–O bond is sufficiently strong (>118 kcal/mol), we believed that the oxygen ligand did not participate in the reaction, as is the case with cyclopropane [23]. However, it is likely that the right answer can be obtained with the use of the $CH_3{}^{18}OH$ methanol.

Reactions of MoO_2^+

The reactivity of MoO_2^+ is much higher than the reactivity of MoO^+. MoO_2^+ also entered methanol dehydrogenation reactions, which occurred with the elimination of both formaldehyde and water. The $MoO_2CH_2^+$ product can exhibit two different structures: the coordinated formaldehyde OMo^+–CH_2O and the carbene species O_2Mo^+=CH_2. The collisional activation of this product resulted in the formation of Mo^+ (35%), MoO^+(50%), and $MoCH_2O^+$(15%). These data unambiguously suggest the presence of two ligands in the structure, oxygen and formaldehyde. Thus, methanol dehydrogenation occurs by the activation of the C–H or O–H bond of methanol.

Data given in Table 3 demonstrate that, as distinct from Mo^+ and MoO^+, the MoO_2^+ ions can be inserted into the C–O bond of methanol. The $MoO_2CH_3^+$ and $MoO_2CH_4^+$ ions are the main products of this insertion. The formation of these products from MoO_2^+ was found using the double resonance technique.

Table 4. Ionization potentials (*PI*) and the energies of C–H, C–O, O–H, and C–C bonds in alcohol molecules

Bond	Energy, kcal/mol [24]	*IP*, kcal/mol
CH_3–OH	91.6	254
CH_3O–H	102.4	
H–CH_2OH	91.7	
C_2H_5–OH	91.1	244
C_2H_5O–H	101.5	
$CH_3CH(OH)$–H	90.2	
CH_3–CH_2OH	85.1	
$C_2H_5CH(CH_3)$–OH	91.3	235
$C_2H_5CH(CH_3)O$–H	102.1	
$C_2H_5CH(OH)$–CH_3	86.5*	
C_2H_5–$CH(OH)CH_3$	77.7	
$(CH_3)_3C$–OH	92.7	227
$(CH_3)_3CO$–H	103.8	
CH_3–$C(CH_3)_2OH$	81.2*	

* Data from [18].

Other Oxides

The main reaction of MoO_3^+ is the formation of $MoO_3CH_3^+$ ions, because one oxygen ligand in the MoO_3^+ ion has a free valence, which is responsible for its higher reactivity. The interaction with the CH_3 group results in the occupancy of this vacancy, and the reaction is strongly exothermic. The reaction can occur via the insertion of the Mo^+–O fragment into the C–H or C–O bond of methanol. The tendency for ions with the general stoichiometry MoO_3^+ to form $Mo_xO_yCH_3^+$ is retained. The participation of structurally similar MoO_3^+ and $Mo_2O_6^+$ ions in the reaction resulted in almost identical reaction products. However, the reactivity of cyclic $Mo_3O_9^+$ ions is dramatically different from that of other oxide ions.

The reaction occurring with the loss of a water molecule is the main reaction of $Mo_2O_4^+$ ions. This fact suggests that the more bulky the oxide ion, the more preferable hydrogen atom transfer to the oxygen ligand, which results in the formation of H_2O.

Coordinatively unsaturated ions with the general stoichiometry $Mo_xO_{3x-1}^+$, namely, MoO_2^+, $Mo_2O_5^+$, and $Mo_3O_8^+$, exhibited similar linear structures and almost the same reactivity. Only insignificant differences were observed. Thus, the insertion into the C–O bond of methanol is a predominant process for $Mo_2O_5^+$ and $Mo_3O_8^+$ ions. However, the fraction of the $Mo_xO_yCH_4^+$ product increased with the number of molybdenum atoms in the ion. It is likely that the loss of an oxygen

ligand occurred more easily because of a decrease in the M^+–O bond energy with oxide size.

Generally, molybdenum oxide ions are usually inserted into the C–O bond of methanol rather than the C–H bond, as well as the Mo^+ ion. The greater the number of oxygen atoms attached to the molybdenum ion, the greater the amount of products of the reactions that occur via initial insertion into the C–O bond. The insertion of the metal ion or a metal oxide into the O–H bond of methanol can result in the same reaction products as in the case of insertion into the C–H bond. However, in our opinion, the insertion into the O–H bond can be energetically unfavorable because this bond is the strongest bond in the molecule of methanol (Table 4 summarizes data on the energies of C–H, C–O, C–C, and O–H bonds in alcohol molecules). Therefore, in the subsequent discussion, the reactions are considered to occur via initial insertion into the C–H and C–O bonds of alcohols. Scheme 1 illustrates a conceivable reaction mechanism.

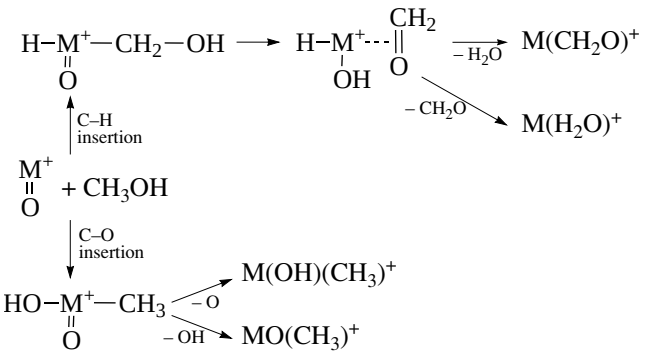

Scheme 1.

The insertion into the C–O bond is accompanied by the formation of the $Mo_xO_y(CH_3)(OH)^+$ intermediate. The elimination of one of the ligands (OH or O) results in the formation of a final product of the reaction.

To test the proposed mechanism, the reactions of molybdenum oxide ions with the isotopically substituted methanol CD_3OH were studied. Table 3 summarizes the distribution of reaction products. The same products as in the reaction with CH_3OH were detected. The formation of a product such as $Mo_xO_yCD_3H^+$ fully confirmed the proposed mechanism.

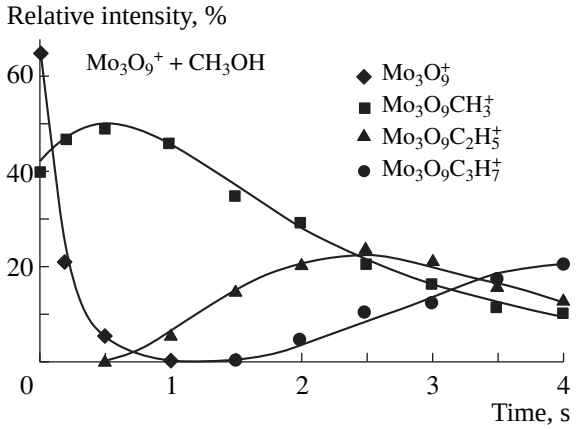

Fig. 3. Kinetic curves of methanol polycondensation on the $Mo_3O_9^+$ cluster.

Polycondensation Reactions

It was found that $Mo_3O_9^+$ ions exhibit unique reactivity. They can consecutively react with several molecules of methanol to form polycondensation products:

$$Mo_3O_9^+ + 2CH_3OH \longrightarrow Mo_3O_9C_2H_5^+ + H_2O + {}^{\bullet}OH, \quad \text{(XII)}$$

$$Mo_3O_9^+ + 3CH_3OH \longrightarrow Mo_3O_9C_3H_7^+ + 2H_2O + {}^{\bullet}OH. \quad \text{(XIII)}$$

Table 5. Theoretical and experimental rate constants of the methanol polycondensation reactions

$$Mo_3O_9^+ \xrightarrow{k_1} Mo_3O_9CH_3^+ \xrightarrow{k_2} Mo_3O_9C_2H_5^+ \xrightarrow{k_3} Mo_3O_9C_3H_7^+$$

$$Mo_3O_9^+ \xrightarrow{k_1'} Mo_3O_9CD_3^+ \xrightarrow{k_2'} Mo_3O_9C_2D_5^+ \xrightarrow{k_3'} Mo_3O_9C_3D_7^+ \xrightarrow{k_2''} Mo_3O_9C_3H_5D_2^+$$

$k_i \times 10^{-10}$, cm^3/s	Experimental	Calculated	k_{expt}/k_{teor}
k_1	1.2	7.8	0.15
k_2	0.93	7.8	0.12
k_3	0.12	7.7	0.02
k_1'	1.07	7.4	0.14
k_2'	0.67	7.4	0.09
k_2''	0.33	6.6	0.05
k_3'	0.08	7.3	0.01

The $Mo_3O_9C_2H_5^+$ product was structurally characterized with the use of the collisional activation of ions, which resulted in fragmentation. The main fragments were $Mo_3O_8C_2H_5^+$ (22%), $Mo_3O_8^+$ (22%), $Mo_3O_8H^+$ (18%), $Mo_3O_9C_2H_4^+$ (15%), $Mo_3O_9^+$ (9%), and $Mo_3O_9H^+$ (6%), as well as cluster degradation products. Thus, the conclusion that one hydrocarbon ligand (C_2H_5 or C_2H_4) rather than CH_3 fragments is the constituent of $Mo_3O_9C_2H_5^+$ can be drawn from the data.

The above reactions are the polycondensation of methanol molecules, which occurs on the molybdenum oxide ion (Fig. 3). Note that similar reactions are well known for homogeneous and heterogeneous catalysts containing molybdenum trioxide, such as heteropoly acids, and for zeolites [37–42]. Table 5 summarizes the rate constants of polycondensation and the constants calculated using the Langevin–Gioumousis–Stevenson theory. A comparison between the experimental and theoretical values demonstrated that the reaction did not occur at every collision.

The interaction of $Mo_3O_9^+$ with CD_3OH also gave the products of deuteriomethanol polycondensation. Ions that contained only deuterium were mainly formed: $Mo_3O_9C_2D_5^+$ and $Mo_3O_9C_3D_7^+$. It is likely that in these ionic species one deuterium atom can be readily exchanged for hydrogen in collision with methanol molecules because the spectra exhibited the following products after a short time (~0.2 s): $Mo_3O_9C_2D_4H^+$ and $Mo_3O_9C_3D_6H^+$.

The question of the mechanism of formation of the first C–C bond in the interaction of two methanol molecules in the presence of a catalyst is still an open question. Various mechanisms were proposed: from a carbene mechanism to a free-radical mechanism [37–42]. The participation of an active C_1 intermediate in cationic form seems most likely [43].

It is believed [42] that Brønsted acid sites are responsible for the transformations. According to the mechanism proposed by Ono and Mori [40], the first carbon bond is formed via a pentacoordinated intermediate in accordance with Scheme 2.

$$CH_3OH + [H]^+ \longrightarrow [CH_3]^+ + H_2O,$$

$$[CH_3]^+ + CH_3OR \longrightarrow \left[\begin{array}{c} H \\ \cdots CH_2OR \\ CH_3 \end{array}\right]^+ \xrightarrow{-H^+} CH_3CH_2OR \xrightarrow{-ROH} CH_2CH_2$$

Scheme 2.

In our case, it is likely that charge transfer to a carbon atom with the formation of a Mo–O–H intermediate can occur with bulky molybdenum oxide ions. In this intermediate, charge transfer to the hydrogen makes it more reactive. The possibility of this transfer was supported by the high proton affinity of molybdenum oxides with the stoichiometry MoO_3. As demonstrated above, these oxides can undergo protonation in a gas phase in the presence of $CH_3OH_2^+$ ions (*PA* of methanol is 186 kcal/mol) according to reaction (XV).

$$CH_3OH^+ + CH_3OH \longrightarrow CH_3OH_2^+ + CH_3O, \quad \text{(XIV)}$$

$$Mo_xO_y + CH_3OH_2^+ \longrightarrow Mo_xO_yH^+ + CH_3OH. \quad \text{(XV)}$$

Moreover, the ionization potentials of alcohols and molybdenum oxides are significantly different (data in Tables 1, 4); charge transfer from an oxymetallic center to an alcohol molecule is exothermic by 23–50 kcal/mol. The hypothesis about possible proton transfer was also supported by the exchange of only one deuterium atom for hydrogen. In a condensed phase, a carbocation can also be formed because of proton transfer. It is well known that the proton can also facilitate the formation of alkanes and alkenes from alcohol molecules [44].

Based on the experimental data, we proposed a mechanism for the formation of the C–C bond in a gas phase. The first step of the proposed mechanism, which is presented in Scheme 3, is the formation of a carbocation. Next, the interaction of the carbocation with the methanol molecule results in chain propagation.

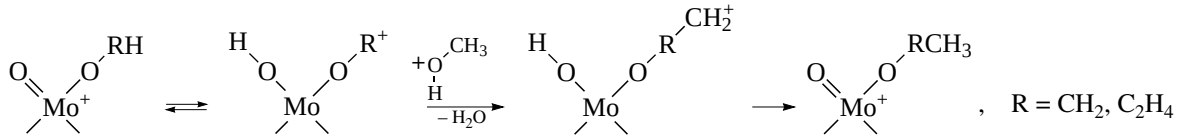

Scheme 3.

The mechanism that includes methanol dehydration with the formation of carbene (CH_2:) is an alternative to the proposed mechanism. This mechanism was invoked previously to explain methanol conversion on zeolites [43].

The corresponding intermediate $Mo_3O_9(CH_2)^+$ was also detected in a gas phase (Table 3); however, this is not the main reaction path. The removal of this primary product using the double resonance technique did not affect the concentration of secondary products.

An intriguing question is the question of why only $Mo_3O_9^+$ ions can enter the reaction with several methanol molecules. As mentioned above, two main factors—energetic and geometric—are responsible for the reactivity of heterogeneous catalysts containing molybdenum trioxide. The $Mo_3O_9^+$ ions have a low binding energy with oxygen; because of this, oxygen can participate in reactions, as was also observed in other bulky oxide ions. However, $Mo_3O_9^+$ exhibits a unique structure: all the atoms are very compactly arranged, bearing a resemblance to a part of a surface. Because of this, in the reaction with two methanol molecules, they can be arranged in the most favorable manner, which is impossible in the case of lighter oxide ions.

Reactions with Ethanol

Previously [18], the interaction of Mo^+ ions with ethanol was studied. It was found that Mo^+ ions enter only the reactions of single and double dehydrogenation of ethanol. The fraction of the single-dehydrogenation products $MoC_2H_4O^+$ was 40%. The products of alcohol dehydration (i.e., insertion into the C–O bond) and C–C bond cleavage were not detected. Thus, Mo^+ was specifically inserted into the C–H or O–H bond of ethanol. Data in Table 4 indicate that the C–H bond (90.2 kcal/mol) in ethanol is somewhat stronger than the C–C bond (85.1 kcal/mol); however, insertion into the C–C bond did not occur. It is likely that the predominant cleavage of the C–H or O–H bond was due to the formation of more highly stable intermediates and products because $D_0(M^+–OH)$ is usually greater than $D_0(M^+–CH_3)$ [45].

Table 6 summarizes the test reactions of $Mo_xO_y^+$ with ethanol and the distribution of reaction products. Molybdenum oxide ions react with ethanol via four main reaction paths: acetaldehyde elimination, single and double dehydrogenation, and formation of the $Mo_xO_yC_2H_5^+$ ion. Almost the same products (acetaldehyde, water, diethyl ether, and ethylene) were detected in a study of ethanol conversion on a heterogeneous catalyst containing molybdenum oxides [46]. Acetaldehyde (96%) was the predominant product of reactions that occurred on MoO_3, whereas ethanol dehydration was the main process in reactions that occur on heteropoly acids [46–48].

Reactions of MoO^+

As in reactions with methanol, MoO^+ reacts with ethanol to form the $MoOH_2^+$ product and to eliminate an acetaldehyde molecule. However, the spectrum also exhibited $MoOC_2H_4^+$ product ions. There are two different structures of this ion: first, an aldehyde molecule coordinated to the molybdenum ion and, second, ethylene coordinated to the molybdenum ion and an oxygen ligand. The activation of $MoOC_2H_4^+$ resulted in the appearance of MoO^+ ions and $MoC_2H_4^+$ traces in the spectra. Thus, the product contained the ethylene molecule; that is, the reaction of ethanol dehydration took place. It is most likely that the oxygen ligand did not participate in the reaction because of the strong Mo^+–O bond. The participation of the oxygen ligand can be determined more accurately with the use of the isotopically substituted ethanol $C_2H_5{}^{18}OH$.

Other Oxides

Both $Mo_xO_{y-1}(H_2O)^+$ and $Mo_xO_yC_2H_4^+$ ions were formed in the interaction of other oxides with ethanol.

Table 6. Distribution of products (%) in the reactions of $Mo_xO_y^+$ ions with ethanol

Reaction products	MoO^+	MoO_2^+	MoO_3^+	$Mo_2O_4^+$	$Mo_2O_5^+$	$Mo_2O_6^+$	$Mo_3O_8^+$	$Mo_3O_9^+$
$Mo_xO_yH_2^+ + C_2H_4O$	84	38	16	34	24	19	29	34
$Mo_xO_yC_2H_4^+ + H_2O$	16	22	27	28	26	33	21	18
$Mo_xO_{y-1}C_2H_2^+ + 2H_2O$	–	13	27	20	30	48	42	48
$Mo_xO_yC_2H_5^+ + {}^{\bullet}OH$	–	27	30	18	20	–	8	–

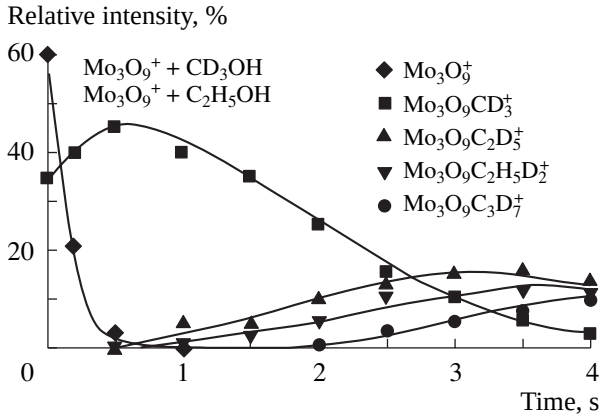

Fig. 4. Kinetic curves of the copolycondensation of CD_3OH and C_2H_5OH on the $Mo_3O_9^+$ cluster.

The structure of these ions is unclear. However, it is well known that Mo^+ selectively dehydrogenates hydrocarbons and alcohols via insertion into the C–H bond. The reactions of molybdenum oxide ions with methanol demonstrated that the presence of oxygen ligands makes preferable insertion into the C–O bond of methanol, especially, in the case of bulky oxides. On the assumption that this is also true of the reactions of $Mo_xO_y^+$ with ethanol, the $Mo_xO_yC_2H_4^+$ ion incorporates the ethylene molecule. The further dehydration of the $Mo_xO_y(C_2H_4)^+$ product can result in the $Mo_xO_{y-1}(C_2H_2)^+$ product, which was observed in the spectra. However, aldehyde dehydration may also result in such a reaction product. The proposed mechanism includes the insertion of the $Mo_xO_y^+$ ion into the weakest C–H bond of ethanol. Next, β-hydrogen transfer from the OH or CH_3 group to the metal ion took place with the formation of a complex with water and acetaldehyde. Water or aldehyde elimination leads to the formation of observed reaction products. Note that the elimination of acetaldehyde was observed in all the molybdenum oxide ions, as distinct from dehydration.

The dehydration of ethanol occurs via insertion into the C–O bond, formation of an ethyl–hydroxide ion complex, and consecutive dehydrogenation of C_2H_5 through β-hydrogen transfer to molybdenum or oxygen. An increase in the size of molybdenum oxide makes the occurrence of double dehydrogenation possible, including the oxide oxygen.

Polycondensation Reaction

Upon the interaction of molybdenum oxide ions with ethanol, ethanol polycondensation products were absent from the spectra. It was found that $Mo_3O_9^+$ ions entered the reactions of ethanol dehydrogenation and dehydration. However, the product $Mo_3O_9C_2H_5^+$ of insertion into the C–O bond was not formed in this case. Previously, it was found that, in the reactions with methanol, the similar product $Mo_3O_9CH_3^+$ is a key intermediate in polycondensation. Thus, the polycondensation reaction did not occur because $Mo_3O_9C_2H_5^+$ was not formed.

Additional experiments were performed with a C_2H_5OH–CD_3OH mixture. Figures 3 and 4 demonstrate the kinetic curves of formation of the products of methanol polycondensation and methanol and ethanol copolycondensation.

As found previously, the $Mo_3O_9CD_3^+$ ions were formed in the reactions with CD_3OH. Next, the resulting product can react with both methanol molecules (reaction (XVI)) and ethanol molecules (reaction (XVII)) to form various polycondensation products:

$$Mo_3O_9CD_3^+ + CD_3OH \longrightarrow Mo_3O_9C_2D_5^+ + HDO, \quad \text{(XVI)}$$

$$Mo_3O_9O_3^{CH} + C_2H_5OH \longrightarrow Mo_3O_9C_3H_5D_2^+ + HDO. \quad \text{(XVII)}$$

The reaction of $Mo_3O_9CD_3^+$ ions with ethanol can also occur by the mechanism shown in Scheme 3.

Reactions with Butanols

Table 7 summarizes the distribution of products of the reactions of molybdenum oxide ions with 2-butanol and 2-methyl-2-propanol (*tert*-butanol). The main reaction of $Mo_xO_y^+$ ions is alcohol dehydration. The cleavage of the C–C bond was also observed. This reaction path appeared as the length of the hydrocarbon chain in the alcohol molecule increased and in the presence of a branched chain.

In the reactions of Mo^+ with butanols, a change in the position of the hydroxyl group decreased the specificity of the reactivity of metal ions [18]. An 80 : 20 ratio between alcohol dehydration and dehydrogenation products was observed in the reactions of Mo^+ with 1-butanol, whereas 50 : 50 and 15 : 85 ratios were observed in the reactions with 2-butanol and 2-methyl-1-propanol, respectively. The products of insertion into the C–C bond were present in insignificant amounts.

As mentioned above, the strong Mo^+–O bond does not allow the oxygen ligand to participate in reactions. Thus, the MoO^+ ions exhibited the same reactivity as the Mo^+ ions. The main processes are the reactions of alcohol dehydrogenation and dehydration. However, in the reaction with *tert*-butanol, about 30% of the products were $MoOCH_3^+$ ions, the products of C–C bond cleavage.

The other molybdenum oxide ions reacted with 2-butanol via three main paths.

First, all the $Mo_xO_y^+$ ions react with the formation of an aldehyde molecule. Second, the coordinatively unsaturated ions of molybdenum oxides (MoO_2^+, $Mo_2O_4^+$, $Mo_2O_5^+$, and $Mo_3O_8^+$) can be inserted into the C–C bond to form $Mo_xO_yCH_3^+$ and $Mo_xO_yC_2H_5^+$. Although the C–C bond in butanols is the weakest (data in Table 4), the fraction of these ions was no higher than 20–30% of the total ion current.

Finally, molybdenum oxide ions enter the reactions of alcohol dehydrogenation and dehydration, and up to three water molecules can be formed in the case of bulky oxides. Oxygen ligands actively participated in all of these reactions. It is likely that repeated dehydrogenation occurs consecutively and is an exothermic process.

Note that under conditions of ICR experiments the released energy can be retained in reaction products as kinetic, vibrational, or electronic excitation. This excitation can accelerate consecutive slow steps. In contrast, on solid supports, relaxation processes occur very rapidly, so that the energy of an exothermic step cannot be used for performing the subsequent endothermic steps [49].

Some distinctions between the reactions of molybdenum oxide ions with *tert*-butanol and 2-butanol were observed. The spectra also exhibited the products of aldehyde elimination, C–C bond cleavage, dehydrogenation, and dehydration. In this case, dehydrogenation was not the main reaction path. Moreover, new reaction paths associated with the formation of the methanol molecule appeared. The formation of products such as $Mo_xO_yC_3H_6^+$ and $Mo_xO_{y-1}C_3H_4^+$ can be explained by the transfer of the CH_3 group in the course of reaction.

Table 7. Distribution of products (%) in the reactions of $Mo_xO_y^+$ with butanols

Alcohol	Reaction products	MoO^+	MoO_2^+	MoO_3^+	$Mo_2O_4^+$	$Mo_2O_5^+$	$Mo_2O_6^+$	$Mo_3O_8^+$	$Mo_3O_9^+$
iso-C_4H_9OH	$Mo_xO_yH_2^+ + C_4H_8O$	27	17	71	22	21	38	25	31
	$Mo_xO_yCH_3^+ + C_3H_7O^\bullet$	–	8	–	11	10	–	–	–
	$Mo_xO_yC_2H_5^+ + C_2H_5O^\bullet$	–	12	–	15	18	–	22	–
	$Mo_xO_yC_4H_6^+ + H_2O + H_2$	31	–	–	–	–	–	–	–
	$Mo_xO_yC_4H_4^+ + H_2O + 2H_2$	42	–	–	–	–	–	–	–
	$Mo_xO_{y-1}C_4H_6^+ + 2H_2O$	–	42	17	20	9	19	16	23
	$Mo_xO_{y-1}C_4H_4^+ + 2H_2O + H_2$	–	21	12	32	24	28	29	28
	$Mo_xO_{y-2}C_4H_4^+ + 3H_2O$	–	–	–	–	18	15	8	18
tert-C_4H_9OH	$Mo_xO_yH_2^+ + C_4H_8O$	23	18	15	20	12	22	18	18
	$Mo_xO_yCH_3^+ + C_3H_7O^\bullet$	29	16	–	12	10	–	21	–
	$Mo_xO_yC_4H_8^+ + H_2O$	11	29	27	17	12	17	10	18
	$Mo_xO_yC_4H_6^+ + H_2O + 2H_2$	37	–	–	–	–	–	–	–
	$Mo_xO_{y-1}C_4H_6^+ + 2H_2O$	–	16	37	24	30	28	24	27
	$Mo_xO_yC_3H_6^+ + CH_3OH$	–	13	12	22	24	20	27	27
	$Mo_xO_{y-1}C_3H_4^+ + CH_3OH + H_2O$	–	8	9	5	12	13	–	10

ACKNOWLEDGMENTS

This work was supported by the International Science Foundation (grant nos. RBG 000 and RBG 300).

The author is grateful to A.V. Kikhtenko and E.F. Fialko for their assistance in performing the experiments and for helpful discussions.

REFERENCES

1. Thomas, C.L., *Catalytic Processes and Proven Catalysts*, New York: Academic, 1970.
2. Haber, J., *Proc. of the Third Int. Conf.*, Climax Molybdenum Co.: Ann Arbor, 1979, p. 114.
3. Sheldon, R. and Kochi, J., *Metal Catalysed Oxidation of Organic Compounds*, Academic, 1970.
4. Grande, P., *Catal. Rev. – Sci. Eng.*, 1980, vol. 21, p. 135.
5. Bielanski, A. and Haber, J., *Catal. Rev. – Sci. Eng.*, 1979, vol. 19, p. 1.
6. Stiles, A.B., *Applied Industrial Catalysis*, Leach, B.E., Ed., New York: Academic, 1983, p. 138.
7. Hasimoto, K., Watanabe, S., and Tarama, K., *Bull. Chem. Soc. Jpn.*, 1976, vol. 49, p. 12.
8. Banks, R.L. and Bailey, G.C., *Ind. Eng. Chem., Prod. Res. Dev.*, 1964, vol. 2, p. 170.
9. Calkins, W.H., *Catal. Rev. – Sci. Eng.*, 1984, vol. 27, p. 347.
10. Eller, K. and Schwarz, H., *Chem. Rev.*, 1991, vol. 91, p. 1121.
11. Kikhtenko, A.V., Goncharov, V.B., Momot, K.I., and Zamaraev, K.I., *Organometallics*, 1994, vol. 13, p. 2536.
12. Jackson, T.C., Jacobson, D.B., and Freizer, B.S., *J. Am. Chem. Soc.*, 1984, vol. 106, p. 1252.
13. Kang, H. and Beauchamp, J.L., *J. Am. Chem. Soc.*, 1986, vol. 108, no. 19, p. 5663.
14. Irikura, K.K. and Beauchamp, J.L., *J. Am. Chem. Soc.*, 1989, vol. 111, no. 1, p. 75.
15. Jackson, T.C., Carlin, T.J., and Freiser, B.S., *J. Am. Chem. Soc.*, 1986, vol. 108, p. 1120.
16. Shilling, J.B. and Beauchamp, J.L., *Organometallics*, 1988, vol. 7, p. 194.
17. Cassdy, C.J. and McElvany, S.W., *Organometallics*, 1992, vol. 11, p. 2367.
18. Huang, S., Holman, R.W., and Gross, M.L., *Organometallics*, 1986, vol. 5, p. 1857.
19. Fialko, E.F., Kikhtenko, A.V., Goncharov, V.B., and Zamaraev, K.I., *J. Phys. Chem., B*, 1997, vol. 101, no. 30, p. 5772.
20. Fialko, E.F., Kikhtenko, A.V., Goncharov, V.B., and Zamaraev, K.I., *J. Phys. Chem., A*, 1997, vol. 101, no. 45, p. 8607.
21. Goncharov, V.B. and Fialko, E.F., *Zh. Strukt. Khim.*, 2002, vol. 43, no. 5, p. 839.
22. Goncharov, V.B. and Fialko, E.F., *Zh. Fiz. Khim.*, 2000, vol. 74, no. 5, p. 896.
23. Goncharov, V.B. and Fialko, E.F., *Zh. Fiz. Khim.*, 2001, vol. 75, no. 5, p. 854.
24. *Energii razryva khimicheskikh svyazei. Potentsialy ionizatsii i srodstvo k elektronu* (Chemical Bond Dissociation Energies. Ionization Potentials and Electron Affinity), Kondrat'ev, V.N., Ed., Moscow: Nauka, 1974.
25. Freas, R.B., Dunlap, B.I., Waite, B.A., and Campana, J.E., *J. Chem. Phys.*, 1987, vol. 86, no. 3, p. 1276.
26. Freas, R.B. and Campana, J.E., *J. Am. Chem. Soc.*, 1986, vol. 108, no. 11, p. 4659.
27. Yu, W. and Freas, R.B., *J. Am. Chem. Soc.*, 1990, vol. 112, no. 21, p. 7126.
28. Kikhtenko, A.V., Goncharov, V.B., and Zamaraev, K.I., *Catal. Lett.*, 1993, vol. 21, no. 2, p. 353.
29. Kretzshmar, I., Fiedler, A., Harvey, J., Schroder, D., and Schwartz, H., *J. Phys. Chem.*, 1990, vol. 101, no. 35, p. 6252.
30. Fialko, E.F., *Cand. Sci. (Chem.) Dissertation*, Novosibirsk, 1998.
31. Kretzchamann, I., Fiedler, A., Harvey, J., *et al.*, *J. Phys. Chem. A*, 1997, vol. 101, p. 6252.
32. Kazanskii, L.P., *Dokl. Akad. Nauk SSSR*, 1973, vol. 209, p. 141.
33. Wells, A., *Structural Inorganic Chemistry*, Oxford: Clarendon, 1984, p. 285.
34. Lehman, T.A. and Bursey, M.M., *Ion Cyclotron Resonance Spectrometry*, New York: Wiley, 1976.
35. Walder, R. and Franklin, J.L., *Int. J. Mass Spectrom. Ion Proc.*, 1980, vol. 36, p. 85.
36. Chung, J.S., Miranda, M., and Bennet, C.O., *J. Catal.*, 1988, vol. 114, p. 398.
37. Misono, M., *Cat. Rev. – Sci. Eng.*, 1987, vol. 29, p. 269.
38. Heiba, E.I. and Landis, P.S., *J. Catal.*, 1964, vol. 3, no. 3, p. 471.
39. Kirmse, W., *Carbene Chemistry*, New: York: Academic, 1971.
40. Ono, Y. and Mori, T., *J. Chem. Soc., Faraday Trans. 1*, 1981, vol. 77, no. 9, p. 2209.
41. Anderson, J.R., Mole, T., and Christov, V., *J. Catal.*, 1980, vol. 61, no. 2, p. 477.
42. Chang, C.D., *J. Catal.*, 1981, vol. 69, no. 2, p. 244.
43. Chang, C.D., *Catal. Rev. – Sci. Eng.*, 1983, vol. 25, no. 1, p. 1.
44. Ono, Y., *Catal. Rev. – Sci. Eng.*, 1992, vol. 34, no. 3, p. 179.
45. Simoes, A.V. and Beauchamp, J.L., *Chem. Rev.*, 1990, vol. 90, p. 629.
46. Misono, M., Okuhara, T., Ichiki, T., Arai, T., and Kanda, Y., *J. Am. Chem. Soc.*, 1987, vol. 109, no. 18, p. 5535.
47. Lee, K.Y., Kaneda, K., Mizuno, N., Misono, M., Nakata, S., and Asaoka, S., *Chem. Lett.*, 1988, p. 1175.
48. Iwasawa, YU. and Tanaka, H., *Proc. 8th Int. Congr. on Catalysis*, Berlin, 1984, vol. 4, p. 381.
49. Zhdanov, V.P. and Zamaraev, K.I., *Catal. Rev. – Sci. Eng.*, 1982, vol. 24, no. 3, p. 373.